UDC 621.3.032.26:621.391.6

Virtually Imaged Phased Array

●Masataka Shirasaki

(Manuscript received March 11, 1999)

A Virtually Imaged Phased Array (VIPA) is a simple design of an optical element which shows large angular-dispersion versus wavelength change. It consists of a semi-cylindrical lens and a thin plate of glass on which reflection coatings are formed. Both theory and experiment show that the angular dispersion is ~0.5 degree/nm, which is large enough to demultiplex dense WDM channels. When the VIPA is used in a wavelength demultiplexer, the fiber coupling efficiency, which determines the insertion loss and the crosstalk, is important. The characteristics of the demultiplexer using the VIPA are analyzed. Temperature dependence of the demultiplexing performance is also an important issue. A temperature insensitive design of the VIPA is described. Another application of the VIPA is chromatic dispersion compensation in a fiber transmission line. The scheme for chromatic dispersion device using the VIPA is discussed.

1. Introduction

Optical wavelength division multiplexing (WDM) is one of the most efficient means of optical communication using an optical fiber. In current WDM systems, which have 8-64 WDM channels with a channel spacing of 0.4-1.6 nm (50-200 GHz), a wavelength multiplexer/demultiplexer is a key component. There have been several technologies developed for wavelength demultiplexing. In the practical systems, dielectric multi-layer filter is currently the most commonly used device. However, the film fabrication process requires very high accuracy in both the thickness and the index in each of many layers when the channel spacing becomes less than 2 nm. Optical interferometers, such as Fabry-Perot or Mach-Zehnder interferometers, can split very narrowly spaced wavelengths. An optical fiber Bragg grating is also a type of demultiplexer for a narrow channel spacing. But all the types of the methods described above can separate only two wavelengths and must be cascaded to decompose many channels of different wavelengths. Since recent multi-channel systems use more than 16 wavelengths, those two-wavelength splitters are not practical, unless only small number of channels need to be separated.

To decompose light into paths for many different wavelengths at one time, the use of a diffraction grating is a popular means.[1),2)] A disadvantage of a demultiplexer using a diffraction grating is the relatively large size of the optical path needed for splitting the wavelengths when the channel spacing is narrow. This is due to the small angular dispersion of the diffraction gratings. As a result, the characteristics are sensitive to misalignments of the elements. Another disadvantage of a diffraction grating is the polarization dependence of the diffraction efficiency. This causes a polarization-dependent loss in the multiplexer/demultiplexer. An alternative to this diffraction grating is a waveguide grating device.[3),4)] Similar to a bulk diffraction grating, a waveguide grating has a wavelength-dependent

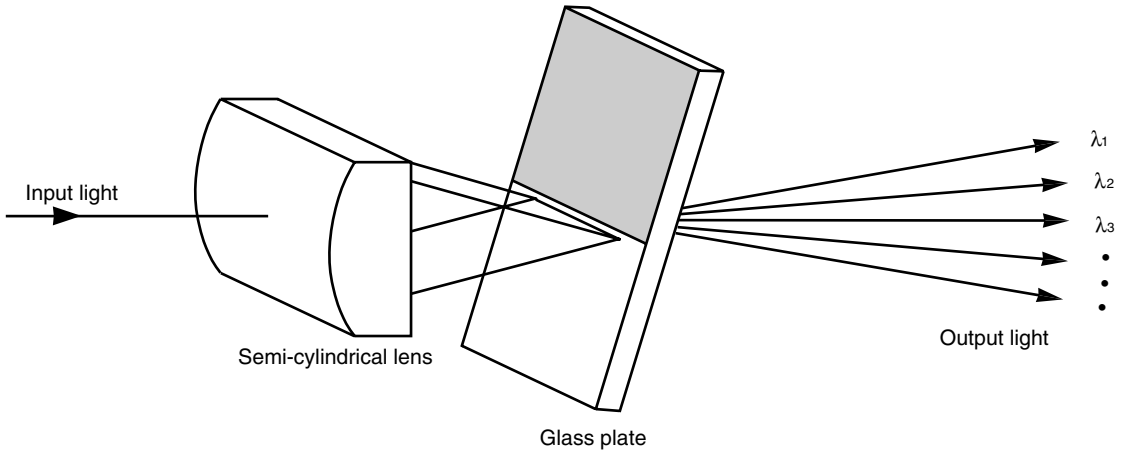

Figure 1
View of VIPA.

diffraction angle (i.e. angular dispersion). This method can generate large angular-dispersion if the waveguide lengths have large differences from one to the next. However, the phase error of the light transmitted through each waveguide must be eliminated and the deviation of the waveguide parameters must be suppressed over the entire substrate. This requires accurate control of the waveguide parameters, such as size, index, and temperature.

Virtually Imaged Phased Array (VIPA) has been developed to generate large angular dispersion.[5),6)] In this paper, an application of the VIPA to a wavelength demultiplexer is discussed as a convenient means and its characteristics are analyzed.

A VIPA has another interesting application, which is the chromatic dispersion compensation of the transmission fiber. There have been two major principles known for chromatic dispersion compensation, which use the dispersion compensation fiber and the chirped fiber Bragg grating.[7),8)] Dispersion compensation fiber has a broad bandwidth, but it shows a large insertion loss and a high optical nonlinear effect. Chirped fiber Bragg grating has relatively narrow bandwidth and cannot cover the entire WDM band. It is known that a diffraction grating produces angular dispersion and that angular dispersion can be converted into chromatic dispersion.[9)] However, the angular dispersion produced by a diffraction grating is too small to compensate for the chromatic dispersion in a transmission fiber. A large angular dispersion produced by the VIPA will be useful in this application.

2. Virtually imaged phased array

VIPA is a simple structure which shows large angular-dispersion as the wavelength changes.[5),6)] The schematic of the VIPA is shown in **Figure 1**. The VIPA employs a thin plate of glass and a semi-cylindrical lens. The input light is line-focused with the semi-cylindrical lens into the glass plate. Then the collimated light emerges from the reverse side of the plate where the light propagates at an angle which varies as the wavelength of the incident light changes. Note that the angular dispersion of the VIPA operates only in the side view. From the top view, the light is simply a collimated light for all the wavelengths.

Figure 2 shows the side view details of VIPA's operation. In Figure 2, the light input side is coated with a 100%-reflection film except in the light incident window which is anti-reflection coated. The light output side of the glass plate is coated with a high-reflection film. The input light, after a semi-cylindrical lens, enters the plate through the window and is line-focused at the

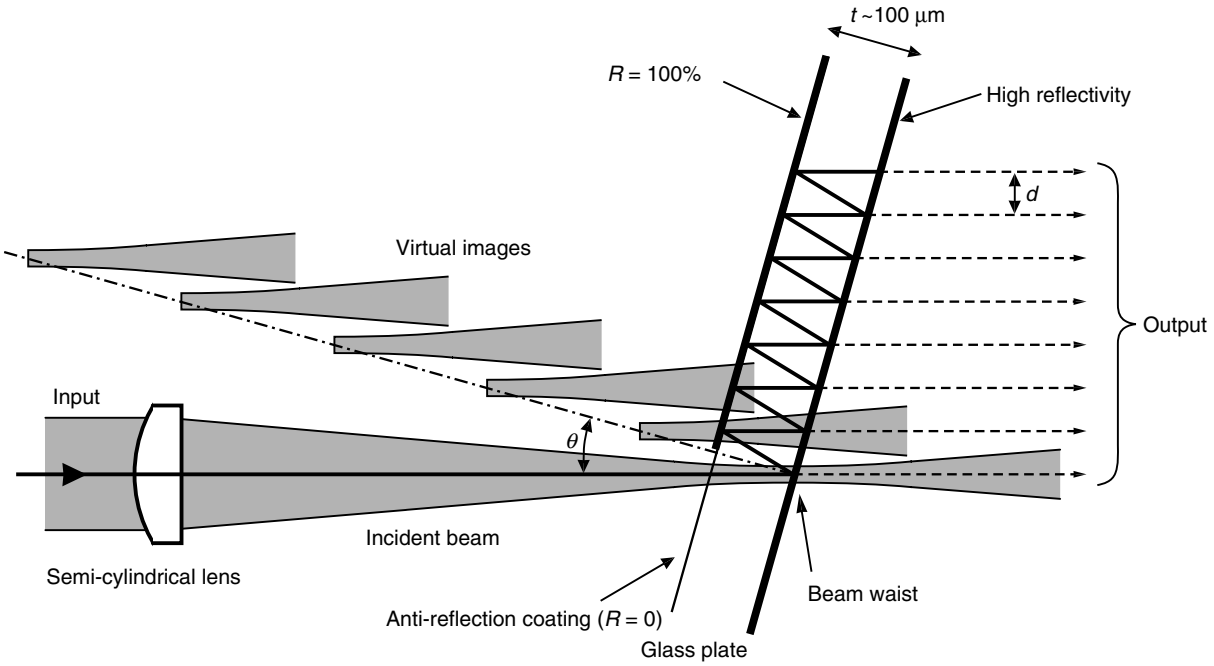

Figure 2
Detailed structure and operation of VIPA in side view.

surface of the output side. Here, the center axis of the input light to the surface has a small incident angle θ. It should be noted that θ is the incident angle within the plate and the refraction at the glass surface is ignored for simplicity. Therefore, the actual incident angle to the plate in the air is about n times larger due to refraction (n is the refractive index of the plate and $n = 1.5$ for glass). A part of the incident light passes through the output surface and diverges after the beam waist, at which point the light is line-focused. The rest of the incident light is reflected and, after the second reflection, hits the same surface but is displaced by d. Then a part of the light passes through the surface. In a similar way, after the plate, the light is split into many paths with a constant displacement d. In Figure 2, the refraction at the output surface is also ignored.

If the reflectivity at the output surface of the plate is uniform over the entire surface, then the beam shape in each path forms as if the light diverges from the virtual image of the beam waist. The virtual images of the beam waist are located with the constant spacing $2t$ (t is the thickness of the plate) along the line which is normal to the plate. The positions of the beam waists in the virtual images are self-aligned and there is no need to adjust individual positions. After exiting the glass plate, all of the beams interfere and then form collimated light, where the light propagates in a particular direction which is determined by the condition of diffraction and is a function of the light wavelength. This output profile is analytically solved as shown below. If the reflectivity at the output surface of the plate is graded along the surface, the beam shape would be distorted through the reflections and the output profile would need to be analyzed numerically.

Assuming the reflectivity is uniform, the spacing of the light paths is $d = 2t\sin\phi$ and the difference in the path lengths between adjacent beams is $2t\cos\phi$. Here, ϕ is the output angle with respect to the normal to the plate as shown in **Figure 3**. Since Figure 3 does not consider the refraction at the surface of the plate, the angles in the air for θ and ϕ appear about n times larger. The angular dispersion is proportional to the ratio of the two numbers described above, which is

$\cot\phi$. The angular dispersion after the plate is also about n times larger because of refraction. Thus, the effective factor which determines the angular dispersion is approximately $n\cot\phi$.

The VIPA is essentially polarization insensitive. A polarization dependence of a VIPA appears only if the reflectivities of the reflection films on the plate have polarization-dependence either in amplitude or phase. But their polarization-dependence can be ignored for a small incident angle below 10 degrees.

3. Angular dispersion

To confirm the large angular dispersion, the output angle of the VIPA was measured. The setup is shown in Figure 3. The parameters used in the experiment, for the 1.55 μm wavelength range, are: t = 100 μm, θ = 6.4 degrees, and therefore d = 22.4 μm, and the output surface of the plate has a uniform reflectivity of 95%. With these numbers, the factor $n\cot\phi$ at the center output angle where $\phi = \theta$ is 13.4. The corresponding factor for a diffraction grating is 2tan(blaze-angle) and this factor for a common blaze angle of ~30 degrees is about 1. Thus, the angular dispersion of the VIPA is much larger than those of gratings. One important design issue in a VIPA is the need to ensure that the input light passes through the window area and that the light is incident on the 100%-reflection area after the first reflection. This requirement determines the minimum angle θ. When the beam waist size is 10 μm, the beam size on the window, which is about 100 μm away from the beam waist in the glass, is 12 μm. Then θ must be larger than 3.5 degrees in order to reflect most of the light on the rear mirror area. The θ used in the above experiment satisfies this condition.

The input light from a wavelength-tunable laser-diode in the 1.55 μm range was introduced through a single mode fiber and collimated with a lens as shown in Figure 3. The light was then line-focused with a semi-cylindrical lens. First, it was confirmed that the output light from the glass plate was well collimated. The beam divergence was very small and the diameter measured at a distance of 20 cm from the glass plate was about 0.6 mm. Next, the output angle with respect to the light incident direction, which is $\Phi = n(\phi - \theta)$ was measured. When the wavelength was changed, Φ changed very sensitively. The result is shown in **Figure 4**. It appears that the curve is not linear and the angular-dispersion $|d\phi/d\lambda|$ is larger at smaller Φ (λ is the wavelength). This is because the effective factor for the dispersion, $n\cot\phi$ is larger at smaller Φ. The angular dispersion varies from 0.4 degree/nm to 0.8 degree/nm in the wavelength range of Figure 4. For $\Phi = 0$ or $\phi = \theta$, the angular dispersion is about 0.5 degree/nm and this value has good agreement with the theoretical value, $n\cot\theta/\lambda$ in radian/nm.

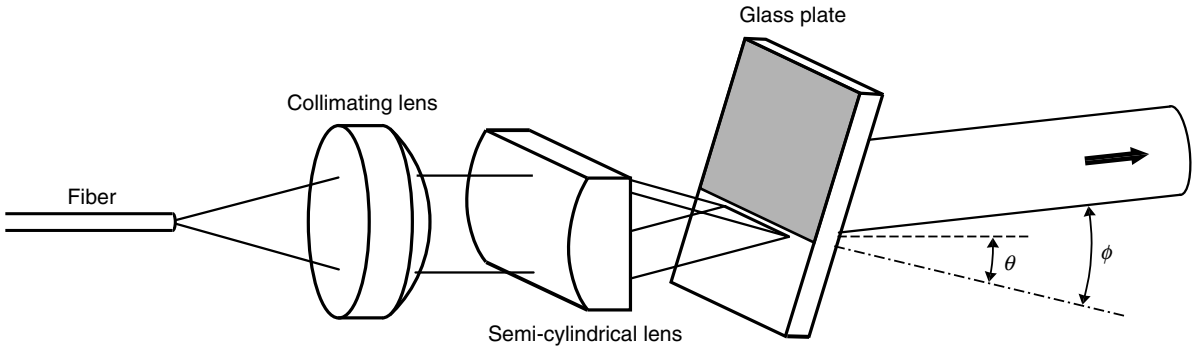

Figure 3
Schematic for measurement of angular dispersion.

4. Demultiplexing characteristics

The large angular-dispersion of the VIPA can be applied to demultiplexing of the WDM channels. The output light of the VIPA traveling in the direction which depends on the wavelength is coupled to the corresponding fiber through the focusing lens as shown in **Figure 5**. In order to analyze the filtering characteristics of the demultiplexer, the output beam profile of the VIPA and then the fiber coupling efficiency must be calculated. In the VIPA with a uniform reflectivity, the field magnitudes of the virtual images decay exponentially as the number of reflections increases. The decay rate of amplitude in one round trip in the VIPA plate is the square root of the reflectivity, which is ~0.975 when the reflectivity is 95%. Assuming that the reflectivity does not vary within the vicinity of the incident angle, the beam profiles in all of the light paths are the same because they are the virtual images created through the mirrors. Therefore, assuming that all of the beams diverging from the corresponding virtually-imaged beam waists have the same profile and that their magnitudes are constant in the vicinity of the direction which satisfies the condition of diffraction, the output field traveling in the direction at a deviation angle $\Delta\phi$ (in radian) from the diffraction angle is proportional to $1/(1-e^{-\alpha+ikd\Delta\phi}) \simeq 1/(\alpha-ikd\Delta\phi)$. Here, $k = 2\pi/\lambda$ and $e^{-\alpha}$ is the square root of the film reflectivity, which is 0.975 for 95% reflectivity. The approximation is valid for small α and small $kd\Delta\phi$, and thus the output is Lorentzian.

The filtering characteristics are evaluated by using a two dimensional model in the plane of Figure 2. As shown in Figure 5, the output light is coupled to a single mode fiber with a focusing lens (the focal length is f). When the vertical displacement of the lens is h, the field pattern in the lens focal plane is $e^{ikh\Delta\phi}/(\alpha-ikd\Delta\phi)$, where $f\Delta\phi$ is the distance along the focal plane. The fiber coupling efficiency is the square of the overlap integral between the output field pattern in the lens focal plane and the waveguide mode in the fiber, which

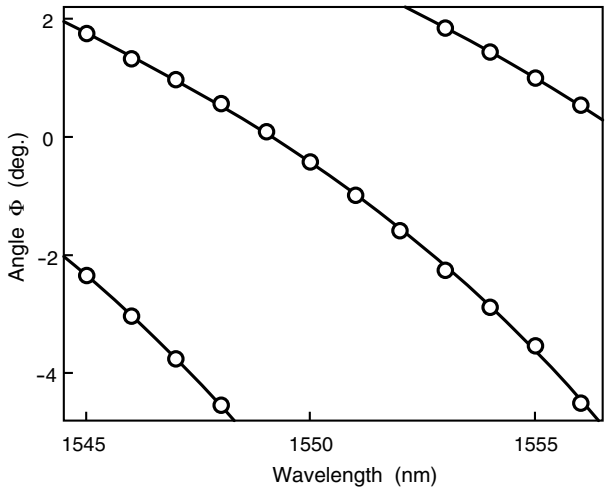

Figure 4
Output angle vs. Wavelength.

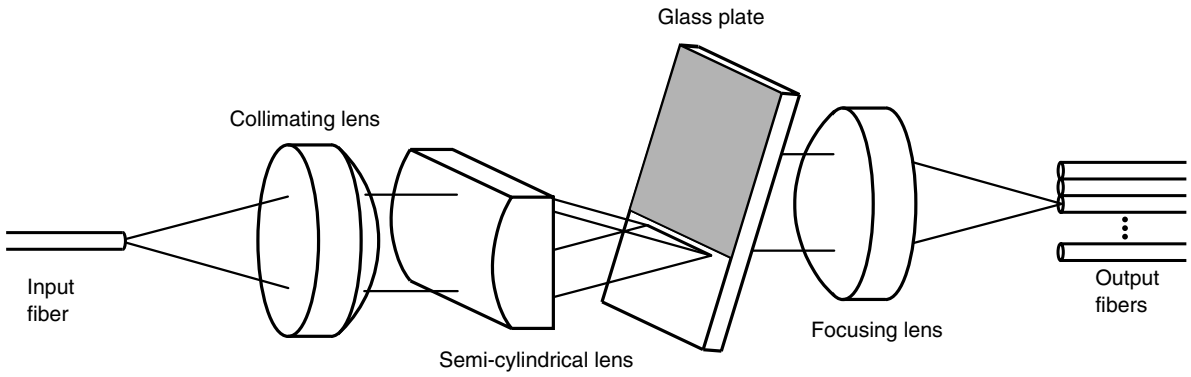

Figure 5
Design of VIPA demultiplexer.

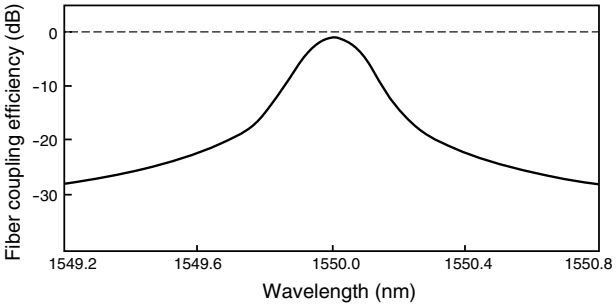

Figure 6
Coupling efficiencies to output fiber.

we model with a Gaussian profile. Here, h is optimized so that the coupling efficiency is maximized. Assuming $e^{-\alpha}$= 0.975, θ= 4.3 degrees, and f = 35 mm, the fiber coupling efficiency is calculated as shown in **Figure 6**. The insertion loss is 1.0 dB (~80% coupling efficiency), and the crosstalk is −23 dB at wavelengths which are three times the 3 dB bandwidth away from the center wavelength. The crosstalk is not well suppressed and this is due to the slowly decaying tails of the Lorentzian output profile. Therefore, suppression of crosstalk is critical in designing the VIPA.

To improve the characteristics, we modify the output field profile by using a graded reflectivity along the output surface of the glass plate. The reflectivity is high (100%) where the incident beam first strikes the output surface, then gradually decreases along the output surface. This allows almost no transmitted light from the original beam waist, gradually more transmitted light as the reflected beam moves up the plate, and finally less as the reflections lose power. Because of the graded reflectivity, the output beam will have a different shape.

5. Numerical analysis

Since the virtual image model with simple mirrors is not valid with graded reflectivity, a numerical analysis was used. We evaluated a cross-section of the input field at the output surface of the glass plate, recomputed the field profile on the same output surface after the ith round-trip, and then superposed all of the fields to find the output beam profile. Each time in the recomputing process from the ith field to the (i+1)th field, the field was multiplied by the amplitude reflectivity $R_A(y)$ which is a function of the position y along the surface, was Fourier transformed into the spatial frequency domain, was multiplied by the phase factor corresponding to the spatial propagation, and then was inverse Fourier transformed into the space domain. In practice, we end the summation when the magnitude of the field after the ith round-trip falls below a threshold value, typically using ~100 virtual images.

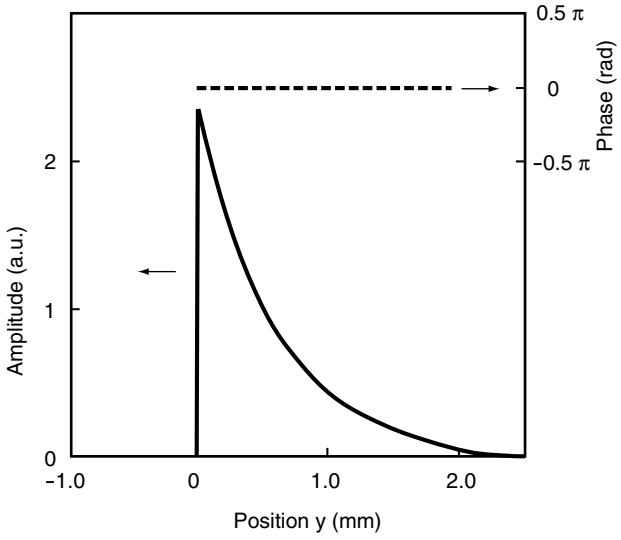

Figure 7
Output beam profile with uniform reflectivity.

The focused output in the lens focal plane is a Fourier transform of the field at the output surface of the glass plate, with linear phase due to vertical displacement h of the focusing lens. We choose h to maximize the fiber coupling efficiency.

First, we used the numerical analysis for the model with the uniform reflectivity of 95%. The amplitude and the phase of the output beam from the plate were obtained as functions of the position y on the surface, and are shown by the solid line and the dashed line, respectively, in **Figure 7**. Here, the linearly changing phase due to the angle between the output beam and the normal to the plate was subtracted. The amplitude is exponen-

tial as expected and the phase is uniform. Using the Fourier transform of this output profile, the fiber coupling efficiency was calculated. The results were almost the same as the analytical results, that is, 1.0 dB insertion loss (80.5% fiber coupling) and –23 dB crosstalk.

Next, the reflectivity at the output surface of the glass plate is gradually changed so that the amplitude transmissivity $T_A(y)$ varies in proportion to the position y. The reflectivity used in the simulation was $T_A(y) = 0.5y$, y in mm. The amplitude and the phase of the output beam from the plate are shown by the solid line and the dashed line, respectively, in **Figure 8**. The phase is uniform and the amplitude profile is closer to a symmetric one than the exponential shape in Figure 7. Using the Fourier transform, the fiber coupling efficiency for this graded reflectivity model was calculated. Losses due to higher-order output beams were not relevant in the comparison and were ignored. By using the graded reflectivity instead of the uniform reflectivity, the maximum coupling efficiency was improved from 80.5% to 99.5%. The crosstalk was reduced from –23 dB to –59 dB at wavelengths which are 3 times the 3 dB bandwidth away from the center wavelength.

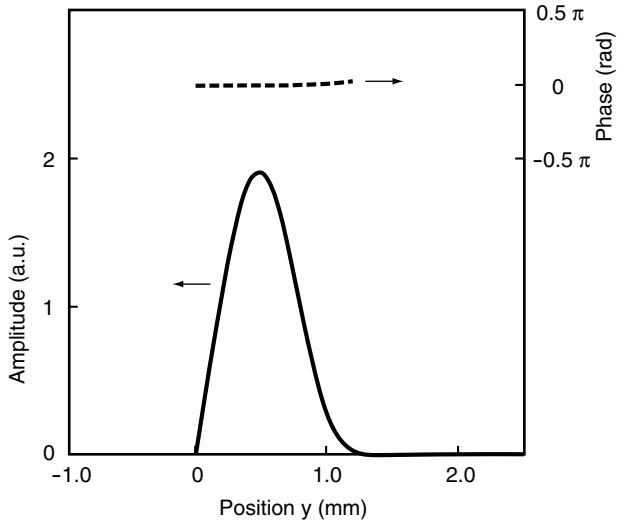

Figure 8
Output beam profile with graded reflectivity.

6. Temperature dependence

The wavelength selected by the demultiplexer for each output fiber using the VIPA element varies if the effective thickness of the glass plate changes due to the temperature change. The effective thickness is the optical length along the light path between the surfaces of the glass plate. Since the optical length is the product of the physical length, which is approximately the thickness of the plate, and the refractive index, the demultiplexed wavelength varies as the temperature changes, if this product changes with temperature change. When the temperature increases, the physical thickness of the plate usually increases due to the thermal expansion. The rate of the thickness increase is α /°C (α is the thermal expansion coefficient). For most optical glass materials, the order of magnitude for α is 10^{-5}. If the refractive index of the plate does not change, the demultiplexed wavelength will change at the rate of α. This causes a shift of the demultiplexed wavelength by 1 nm at 1550 nm wavelength when the temperature changes 60°C. The refractive index also usually increases as the temperature increases. The rate of the increase in refractive index is defined as n_T, where $n_T = (dn/dT)/n$ (n is the refractive index). The typical number for n_T in many glasses is 5×10^{-6}.

The effective thickness varies at a rate which is the sum of the thermal expansion coefficient α and the index change rate n_T. While the thermal expansion is usually positive, the refractive index may decrease or increase as the temperature increases, depending on the material. But the sum of these two coefficients is usually positive. A glass material in which the optical length is insensitive to temperature does not yet exist. Therefore, suppression of the temperature dependence is a very important issue, especially in a device for a narrow channel spacing. Fused silica is one of the most popular materials, and has a low thermal expansion of 0.5×10^{-6}/°C and an index change rate of 8×10^{-6}/°C. Thus, the total tem-

perature coefficient of the effective thickness is 8.5×10^{-6} /ºC. In order to suppress the temperature coefficient, athermal glass, which shows a negative index change rate, can be used instead of fused silica. A typical athermal glass shows a thermal expansion of 11×10^{-6} /ºC and an index change rate of -4×10^{-6} /ºC. Thus, the total temperature coefficient is 7×10^{-6}/ºC. These temperature coefficients in fused silica and the athermal glass are not small enough to be neglected because the demultiplexed wavelength shifts from the designed value (1550 nm) by ~1 nm when the temperature changes by 80ºC. To use the filter in a high density WDM system, which has ~1 nm channel spacing, the temperature coefficient must be less than $\sim 1 \times 10^{-6}$ /ºC.

To suppress the temperature dependence of the VIPA, the new structure shown in **Figure 9** is introduced. A thin plate of glass, which forms the plate of the VIPA, is sandwiched by thick glass plates having anti-reflection coatings on the external facets.[10] The thick plates (outer plates) have a thermal expansion coefficient of α_2. The thin plate (center plate) has a thermal expansion coefficient of α_1, an index change rate of n_T, a Poisson ratio of σ, and two coefficients of the strain-induced index change (i.e. p_1 and p_2, for the strain parallel and perpendicular, respectively, to the optical field). Here, α_2 is greater than α_1. When the temperature increases, α_1 and n_T directly produce a change of optical length in the center plate and this change is usually positive. The other effect is the thermal expansion of the outer plates. Since $\alpha_2 > \alpha_1$, due to the thermal expansion of the outer plates, which is greater than that of the center plate, the center plate is further stretched in the plane by a factor of $(\alpha_2 - \alpha_1)\Delta T$, where ΔT is the temperature change. This stretch decreases the physical thickness of the center plate by the Poisson ratio as shown in **Figure 10**. Because the center plate is stretched in two dimensions, the decrease of the physical thickness is $\sigma_0(\alpha_2 - \alpha_1)\Delta T$, where $\sigma_0 = 2\sigma/(1-\sigma)$. This effect has the negative contribution in the temperature coefficient of the VIPA. Thus, the temperature dependence caused by the change in optical length directly through α_1 and n_T could be canceled by this effect. The three dimensional distortion of the center plate

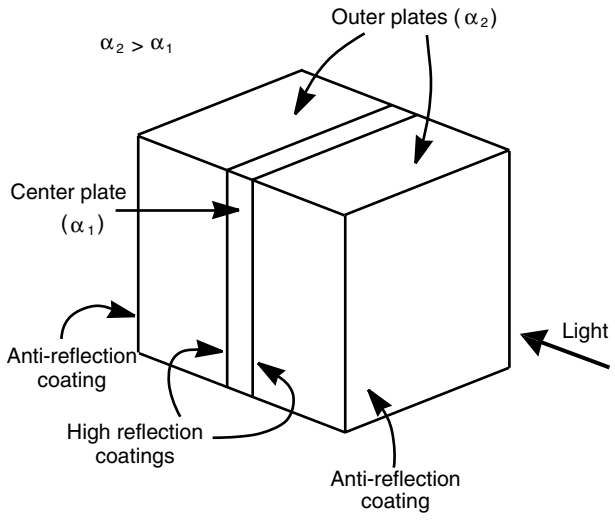

Figure 9
Design of temperature insensitive VIPA.

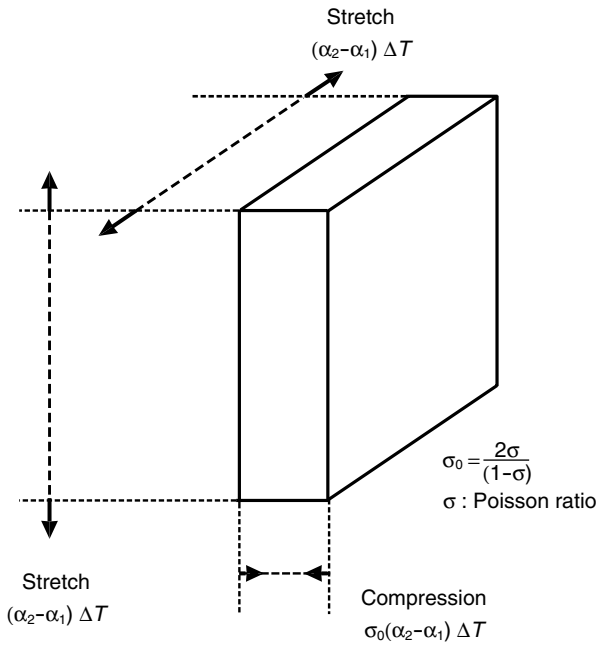

Figure 10
Mechanism of temperature insensitive VIPA.

may produce an index change that is related to p_1 and p_2. Therefore, the temperature coefficient of the optical length is $\alpha_1+n_T-(\alpha_2-\alpha_1)\{\sigma_0+p_1+p_2(1-\sigma_0)\}$. By choosing materials having suitable parameters, this coefficient can be adjusted to zero.

The temperature coefficient of this structure was measured. The materials were selected among common glasses. The outer plates (~1 mm thick each) have a large thermal expansion (α_2 = 14×10^{-6} /ºC). The center plate (~60 μm thick) has $\alpha_1 = 6 \times 10^{-6}$ /ºC, $n_T = 1.5 \times 10^{-6}$ /ºC, $\sigma = 0.3$, and p_1 and p_2 are unknown. With these numbers, and assuming that p_1 and p_2 are zero, the temperature coefficient is 0.6×10^{-6} /ºC. Since p_1 and p_2 are usually small positive numbers, the temperature coefficient may be slightly smaller and is expected to be near zero. The experimental result is shown by the solid line in **Figure 11**. The vertical axis indicates the shift of the demultiplexed wavelength in the 1550 nm wavelength range. The dashed line and the dash-dotted line indicate the temperature dependences (theoretical curves) for fused silica and the athermal glass described above, respectively. The wavelength shift of the improved structure is less than 0.02 nm in the temperature range between 5ºC and 85ºC.

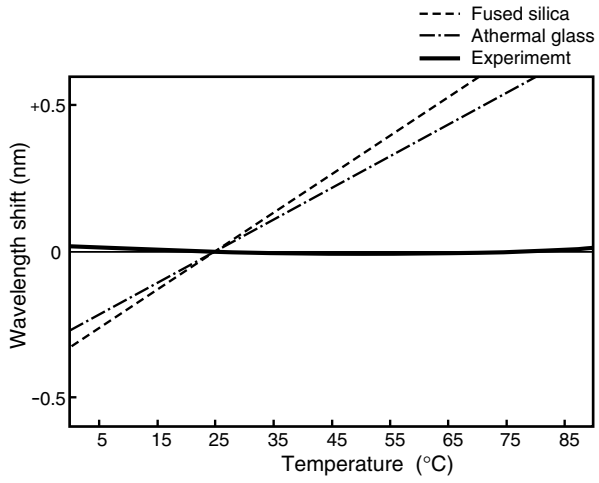

Figure 11
Wavelength shift vs. temperature.

7. Chromatic dispersion compensation using VIPA

The angular dispersion produced by the VIPA can be converted into chromatic dispersion, and therefore, the VIPA technology can be applied to chromatic dispersion compensation in a fiber transmission line.[11),12)] In this application, the VIPA is designed for a very large angular-dispersion to create a negative chromatic dispersion which is large enough to compensate for the positive chromatic dispersion produced in transmission of over 100 km. This large angular-dispersion is obtained by using parameters of the VIPA, which are different from those for demultiplexers. In the discussion below, the thickness t of the plate is 1 mm, and the reflectivity on the plate is 98%. The spacing between the adjacent light paths d in Figure 2 is 50 μm, and the angular dispersion, which is approximately $2nt/d\lambda$ in radians, is 2.2 degree/nm.

The design for the chromatic dispersion compensation is shown in **Figure 12**. The input light from a fiber is collimated with a collimating lens and enters the VIPA. The output light from the VIPA is focused onto a mirror with a focusing lens and is returned through the focusing lens to the VIPA. Since the light is returned to the VIPA in the exactly opposite traveling direction for each wavelength through the focusing lens-mirror-focusing lens path, the returned light is coupled to the input fiber. This returned light is separated for output with an optical circulator. In the experiment, the collimating lens has 6 mm focal length, the semi-cylindrical lens has 20 mm focal length, and the focusing lens has 150 mm focal length.

This scheme creates chromatic dispersion in the following way. We assume that the ray at the center of the output light of the VIPA in Figure 2 comes from a beam waist which is one of the beam waists in the virtual image. This particular beam waist is the one which falls directly on the center line of the output light as extended to the left of the glass plate. It is designed so that the ray at

the center, which travels on the lens axis, is reflected on the mirror at the focal point of the focusing lens, and returns along the lens axis to the beam waist in the virtual image, which is the one the ray comes from. When the wavelength of the light is longer, the output light from the VIPA travels slightly downward in Figure 2. Then, as shown in **Figure 13**, the light is focused at a lower point on the mirror, and the returning light to the VIPA goes to a lower position. When the wavelength is shorter on the other hand, the output light from the VIPA travels slightly upward in Figure 2. Then the light is focused at an upper point on the mirror, and the returning light to the VIPA goes to an upper position. This displacement of the returning light for a 1 nm change of wavelength is $2f$ times the angular dispersion $2nt/d\lambda$. (f is the effective focal length of the focusing lens, which is the actual focal length less the distance from the beam waist at the center to the lens.) The returning light for a longer wavelength goes to the beam waist at a lower position in the virtual image, which has a shorter traveling distance (Figure 13), and the returning light for a shorter wavelength goes to the beam waist at an upper position in the virtual image, which has a longer traveling distance. As a result, the overall distance from the original beam waist to the beam waist to which the light returns along the ray becomes shorter for a longer wavelength and longer for a shorter wavelength. This is a negative chromatic dispersion and the magnitude is $2nt/dc$ times the displacement described above (c is the speed of light). Therefore, the chromatic dispersion is $-8fn^2t^2/d^2c\lambda$.

One important design issue is that the mir-

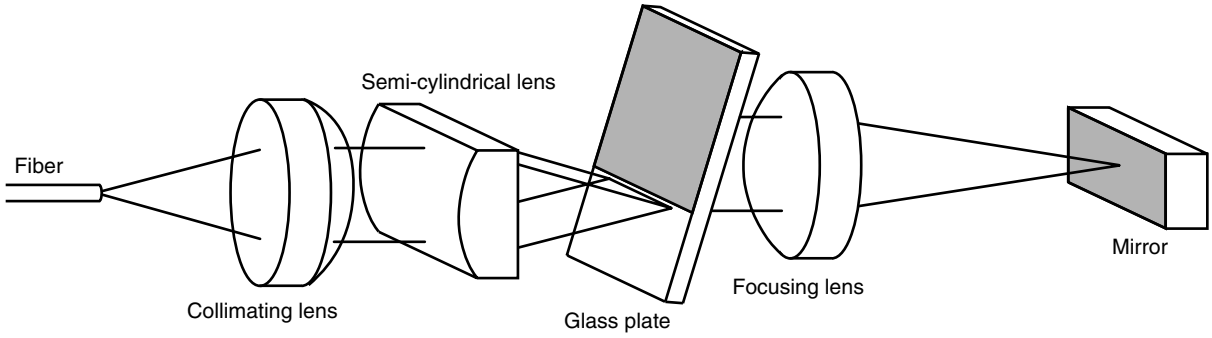

Figure 12
Schematic of chromatic dispersion device.

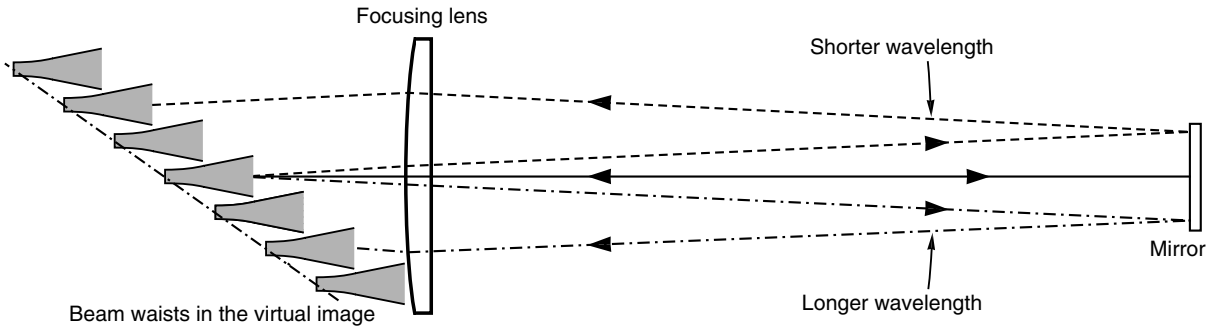

Figure 13
Mechanism of chromatic dispersion generation.

ror in Figure 12 and Figure 13 reflects only the light in a specific order of interference. In the VIPA, one wavelength may have more than one output angle which have different orders of interference. The size and the position of the mirror are designed so that the light in only one order of interference is focused on the mirror and reflected, and that the light in any other order of interference is focused off the mirror.

The design described above was used in an experiment to verify compensation for the chromatic dispersion of transmission fiber in the setup shown in **Figure 14**. First, 10 Gb/s nonreturn-to-zero (NRZ) signals at 1.55 μm wavelength were transmitted with 0 dBm power through a 110 km long standard single mode fiber. An optical amplifier was inserted after 50 km to amplify the power to 0 dBm. When the transmitted light was detected directly with the receiver, the eye diagram was completely collapsed due to the positive dispersion of 1800 ps/nm through thetransmission fiber, as shown in the upper trace of **Figure 15**. Next, the transmitted light was introduced to the VIPA compensation setup. As shown in the lower trace of Figure 15, the eye diagram was clearly recovered through the dispersion compensation.

An important advantage of this method is that it works for many WDM channels simultaneously. The VIPA used in the experiment employs a glass plate with 1 mm thickness, which has a free spectral range of about 100 GHz. Therefore, similar characteristics are repeated with a 100 GHz (~0.8 nm) period. The transmission spectra of this setup are shown in **Figure 16**. The upper trace indicates the details of the transmission curve for individual channels, which shows a 1 dB-bandwidth of about 0.4 nm in each channel. The lower trace indicates the transmission spectrum in the wide wavelength range from 1525-1575 nm. This shows that the losses at the center wavelengths for over 60 channels within the 50 nm wavelength range are almost constant. In this experiment, the overall insertion loss of the setup was 13 dB, mainly due to misalignments. The insertion loss could be theoretically reduced to about 5 dB. The input-polarization dependence was also measured to be less than 0.1 dB.

8. Conclusion

The Virtually Imaged Phased Array was reviewed. Both the theory and the experiment showed that the VIPA had a potential for large angular-dispersion. In application for wavelength multiplexing and demultiplexing, the design with a uniform reflectivity on the surface of the plate had excessive loss and crosstalk. The analysis for the graded reflectivity showed that both the insertion loss and the crosstalk were significantly improved.

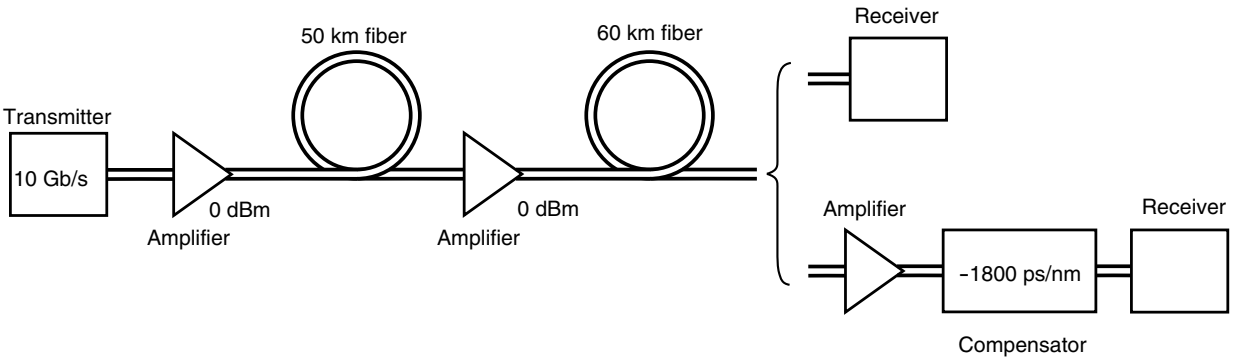

Figure 14
Setup for transmission experiment with chromatic dispersion compensation.

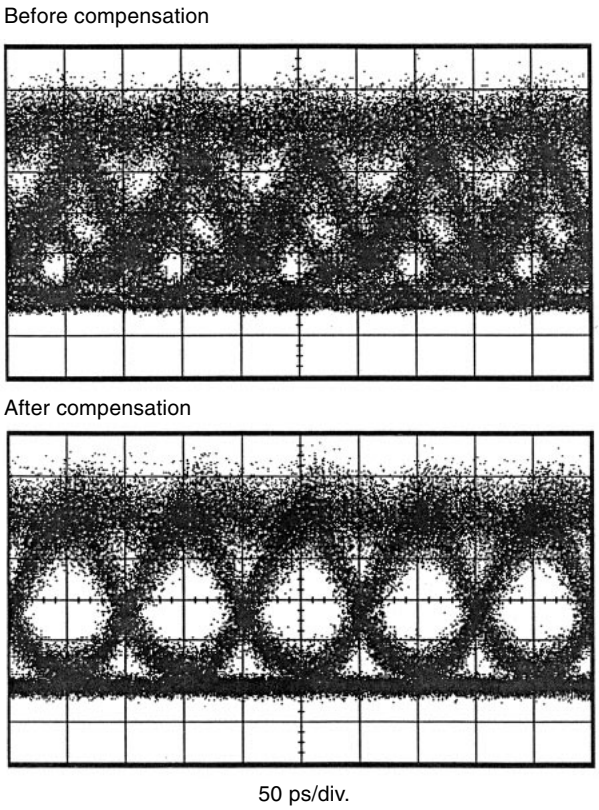

Figure 15
Eye diagrams before and after chromatic dispersion compensation.

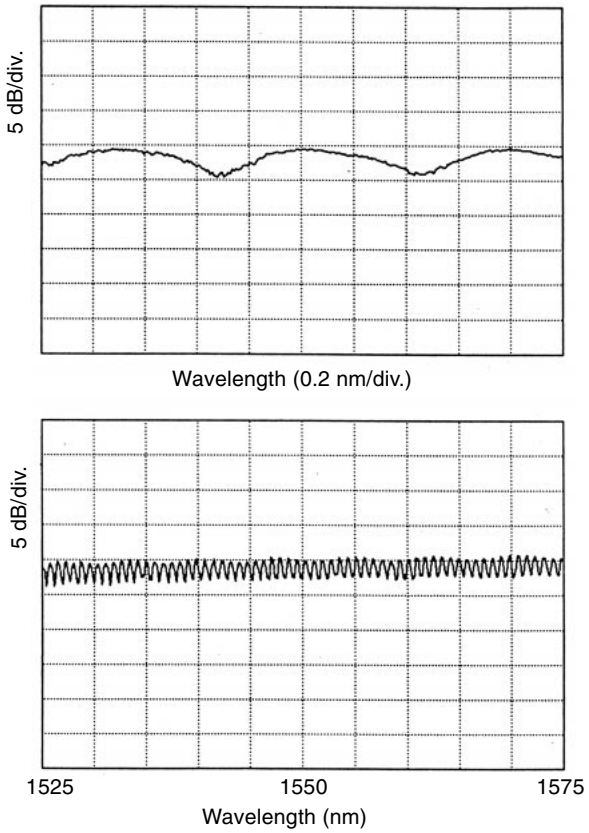

Figure 16
Spectra of chromatic dispersion compensation setup.

A design which suppresses the temperature dependence of the VIPA demultiplexer was described. The experiment showed that the wavelength shift caused by the change of temperature in the range between 5ºC awnd 85ºC was less than 0.02 nm.

The VIPA was applied to compensation for the chromatic dispersion in a transmission fiber. In an experiment with 10 Gb/s data at 1.55 μm wavelength, the chromatic dispersion of ~1800 ps/nm in over 100 km standard single mode fiber was well compensated for.

References

1) J. Lipson, W. J. Minford, E. J. Murphy, T. C. Rice, R. A. Linke, and G. T. Harvey: A six-channel wavelength multiplexer and demultiplexer for single mode systems. *J. of Lightwave Technol.*, **LT-3**, pp.1159-1163 (1985).
2) D. R. Wisely: 32 channel WDM multiplexer with 1 nm channel spacing and 0.7 nm bandwidth. *Electron. Lett.*, **27**, pp.520-521 (1991).
3) M. K. Smit: New focusing and dispersive planar component based on an optical phased array. *Electron. Lett.*, **24**, pp.385-386 (1988).
4) H. Takahashi, S. Suzuki, K. Kato, and I. Nishi: Arrayed-waveguide grating for wavelength division multi/demultiplexer with nanometre resolution. *Electron. Lett.*, **26**, pp.87-88 (1990).
5) M. Shirasaki: Large angular-dispersion by virtually-imaged phased-array (VIPA) and its application to wavelength demultiplexing. Technical Digest, Microoptics Conference (MOC'95), paper PD3, Hiroshima, Japan (1995).
6) M. Shirasaki: Large angular dispersion by a virtually imaged phased array and its

application to a wavelength demultiplexer. *Opt. Lett.*, **21**, pp.366-368 (1996).

7) C. Lin, H. Kogelnik, and L. G. Cohen: Optical-pulse equalization of low-dispersion transmission in single-mode fibers in the 1.3-1.7-mm spectral region. *Opt. Lett.*, **5**, pp.476-478 (1980).
8) F. Ouellette: Dispersion cancellation using linearly chirped Bragg grating filters in optical waveguides. *Opt. Lett.*, **12**, pp.847-849 (1987).
9) O. E. Martinez: 3000 times grating compressor with positive group velocity dispersion: Application to fiber compensation in 1.3-1.6 mm region. *IEEE J. of Quantum Electron.*, **QE-23**, pp.59-64 (1987).
10) M. Shirasaki: Temperature independent interferometer for WDM filters. Technical Digest, European Conference on Optical Communication (ECOC'96), Paper WeD.1.6, Oslo, Norway (1996).
11) M. Shirasaki: Chromatic dispersion compensation using virtually imaged phased array. Technical Digest, Optical Amplifiers and Their Applications (OAA'97), Paper PDP-8, Victoria, BC, Canada (1997).
12) M. Shirasaki: Chromatic dispersion compensator using virtually imaged phased array. *IEEE Photon. Tech. Lett.*, **9**, pp.1598-1600 (1997).

Masataka Shirasaki received the bachelor's, the master's, and the doctor's degrees in Applied Physics from Waseda University, Tokyo, Japan, in 1977, 1979, and 1986, respectively. He joined Fujitsu Laboratories Ltd., Kawasaki, Japan in 1979 and has worked as an optics researcher. During this period, he also worked at Massachusetts Institute of Technology, MA, USA as a Visiting Scientist in 1986-87, 91-94, and 96-present. Currently, he is also a Senior Researcher of Fujitsu Laboratories of America, CA, USA.